Fracture Behaviour of Al-Weldments - Experimental and Numerical Investigations

M. Baur, J.G. Blauel, K. Rädle

Mechanical-technological and fracture mechanics tests have been conducted on real-weld and on weld-thermal-simulated specimens to characterize the effect of material and mechanical heterogeneity (mismatching) on the weld joint behaviour. For the different mismatch ratios produced in welded AlMgSi1 and AlMg4,5Mn plate materials by using different filler materials and heat treatments a strong positive effect on the toughness was found from the developed soft zones. Problems in testing such inhomogeneous weldments and consequences for the defect assessment are discussed.

1. Introduction

Aluminium weld joints are characterized by a high degree of heterogeneity in their material properties and their mechanical behaviour. Especially in the presence of weld defects this will have an effect on the local stress-strain conditions and the local material resistance against crack growth and by that the heterogeneity will influence the global behaviour of a weld joint as well as the load carrying capacity, safety and lifetime of the surrounding structure. As has been shown by the presentations of the 1st International Symposium On Mis-Matching of Welds in Geesthacht (1993) further development of the homogeneous material testing methods, refined numerical analyses based on local stress-strain data and new approaches for an integrated assessment are required to handle such mismatch effects in a quantitative way. A lot of results are available for steel weldments typically with a high strength low toughness coarse grained heat affected zone (HAZ) or an overmatching weld metal (WM; see for example [1]) - here results are presented for aluminium weldments with a characteristic soft HAZ.

Fraunhofer-Institut für Werkstoffmechanik, Freiburg, Germany

2. Materials and Welding; Weld Simulation

The materials used for this study are 25 mm thick rolled plates of the age hardenable alloy AlMgSi1 in the fully hardened condition (T6) and of the non-heat-treatable alloy AlMg4.5Mn in the soft condition. The chemical compositions are given in table 1.

All plates were butt welded using a semiautomatic, multilayer MIG process. Typical parameters were: current 270 A, voltage 28 V, travel speed 0.8 cm/sec, heat input 0.73 kJ/mm. The notch preparation was K-shaped to facilitate fracture mechanics testing. Filler metals AlSi5 and AlMg4.5Mn were used with both base materials (BM) to obtain four different cases of strength mismatch (see table 2). Figure 1 shows a typical weld geometry in a section through the plate thickness.

To study the influence of material property gradients in the HAZ, base material specimens were uniformly treated in a Gleeble 2000 weld simulator by selected and HAZ-representative temperature/time cycles. Four specific points in the HAZ of weld 1 (AlMgSi1/AlSi5) were chosen for simulation (see figure 4a). Tension rod bars and fracture mechanics 3-point-bend specimens were fabricated from such uniformly heat treated material probes and tested in comparison with specimens taken from real welds.

3. Mechanical-technological Material Testing

The extensions of the different HAZs and the degree of softening in the HAZs are characterized by Vicker's microhardness measurements (figure 2). Weld 1 (AlMgSi1/AlSi5) and weld 3 (AlMgSi1/AlMg4.5Mn) show very significant and almost identical hardness minima in the HAZ with a somewhat higher HV for the AlMg4.5Mn weld material. The width of the softened HAZ is about one plate thickness (25 mm).

The hardness in the HAZ can be fully recovered by a post weld heat treatment, which has been carried out for weld 2 (AlMgSi1/AlSi5).

Weld 4 (AlMg4.5Mn/AlMg4.5Mn) shows a uniform hardness level, because BM and WM are of the same alloy and there is no further softening of the BM through welding.

Strength properties of the different zones in the welds were determined by small longitudinal round bar tensile specimens (5 mm diameter, 25 mm gauge length) taken out from different HAZ positions (HAZ 1, HAZ 2, HAZ

3), the BM and the WM. Figure 3 and table 3 show a maximum undermatching of 0.30 for weld 1. The same trends are shown in fig. 4 and table 4 for the weld thermal simulated specimens of the base material AlMgSi1.

4. Fracture Toughness Testing

Specimens and instrumentation:

Deep (a/W = 0.5) and shallow (a/W = 0.1) cracked SE(B)-specimens (20 x 20 mm, 20 x 40 mm) were used to evaluate the material fracture toughness (acc. to [2]). All specimens were notched by spark erosion and fatigue precracked to the desired ratio of a/W before testing.

During loading the force (F), the load line displacement (LLD), and the crack mouth opening displacement (CMOD) were measured and the data stored as well as the DC-potential drop to register crack initiation and stable crack extension.

After the tests and before opening up the fracture surfaces all specimens were fatigue loaded again to mark the end of the stable crack extension.

Evaluation of Data:

The local crack driving parameter J-integral was evaluated from the measured global parameters using the formula proposed by [3,4]:

$$J = \frac{K^2\,(1-\upsilon^2)}{E} + \frac{\eta_c\,A_{pl}}{B(W-a)}$$

with A_{pl} = plastic part of area under the load versus CMOD record, K = stress intensity factor, E = Young's modulus, υ = Poisson's ratio, W = specimen width, B = specimen thickness, a = crack length, η_c =

$$2.632 + 13.687\,(a/W) - 48.847\,(a/W)^2 + 57.979\,(a/W)^3 - 23.343\,(a/W)^4$$

dimensionless factor according to numerical investigations in [3].

This approach has been applied for loading up to initiation and also for limited crack growth. It has been verified especially for shallow cracked specimens (0.05 < a/W < 0.6) and has the advantage of being based on

the measurement of CMOD, which reflects crack tip deformation, rather than on a far field displacement.

Results of Fracture Toughness Tests:

The loss of strength in the HAZ of peak aged AlMgSi1 (see fig. 3) goes in parallel with a gain in toughness. Figure 5a shows crack resistance curves for different AlMgSi1 HAZ materials determined on specimens having experienced a uniform weld thermal heat treatment with different peak temperatures. The toughness level is increased with increasing peak temperature of the simulation cycle which determines the softening (fig. 4).

Crack resistance curves determined on specimens extracted from real welds are compared in figure 5b) for weld 1 and weld 2. The BM of weld 1 and the post weld heat treated (pwht) BM and WM of weld 2 show flat crack resistance curves at a low level (< 20 kJ/m^2). Toughness is much better for WM and HAZ-material in the as welded condition. Maximum toughness is found for a crack positioned in the HAZ 1 of weld 1. This is assumed to be partly due to a strength mismatch effect produced by the global undermatching situation and is being examined by further experiments.

Strength mismatch effects on toughness values are shown in figure 6 by comparing critical J-values determined for WM and HAZ-materials in an undermatched strength situation with those for the same materials in a matched strength situation. For all crack positions examined undermatching leads to a significant increase in the critical toughness values.

5. Numerical Simulations

A two dimensional FE-model has been developed to simulate the loading behaviour of SE(B)-specimens with through thickness cracks under plane strain conditions (fig. 7). Specimens containing a weld are modelled by zones of different flow curves (WM, HAZ 1, HAZ 2, HAZ 3, BM). The parameters varied are material combination (weld 1, weld 2, weld 3), crack position (WM, HAZ 1) and crack depth (a/W = 0.1 and 0.5).

The global (F vs CMOD) and local (J vs CMOD) behaviour of the specimens was studied under increasing displacement. Figure 8a shows results for CMOD = 0.3 mm. For all crack positions in the welds the local loading of the crack tip for a given global deformation is found to be lower compared to the BM. Almost identical values for weld 1 and weld 3 show that the higher WM-strength of weld 3 has a minor influence on the crack

tip loading compared to the overall undermatching situation, which is almost equal for weld 1 and weld 3.

In figure 8b the weld 1 and BM loading behaviour is compared under assumption of stationary cracks. For all displacements the loading of the crack tip is higher in the case of BM. In addition to that the BM crack resistance is lower (fig. 5b).

6. Conclusions

The fracture behaviour of Al-welds is determined by the local toughness as well as by the global strength situation.

The typical soft HAZs and the low strength WMs of AlMgSi-welds reveal better toughness values than the base material.

An overall undermatching in the strength properties of a weld leads to an improved crack resistance compared to a weld with uniform strength.

Literature:

[1] F.M. Burdekin, M. Koçak, K.-H. Schwalbe, R. Denys, "Draft Definitive Statement on the Significance of Mis-match of Strength in Welds", IIW-Doc. X-1282-93

[2] British Standards Institution BS 7448:Part 1:1991, "Method for determination of K_{Ic}, critical CTOD and critical J values of metallic materials"

[3] R.H. Leggatt, J.R. Gordon, "3D elastic-plastic finite element analysis for CTOD an J in SENB, SENA B and SENT specimen geometries", Proceedings of the Conference on Shallow Crack Fracture Mechanics, Toughness Tests and Applications (1992), Cambridge

[4] M.T. Kirk, R.H. Dodds, "J and CTOD estimation equations for shallow cracks in single edge notch bend specimens", Proceedings of the Conference on Shallow Crack Fracture Mechanics, Toughness Tests and Applications (1992), Cambridge

alloy	Si	Fe	Cu	Mn	Mg	Cr	Ni	Zn	Ti
AlMgSi1	1.0	0.31	0.03	0.70	0.79	0.01	0.003	0.025	0.015
AlMg4.5Mn	0.3	0.26	0.07	0.61	4.53	0.11	0.002	0.151	0.016

Table 1: Chemical composition of base materials

weld no.	base material	weld material	remark
1	AlMgSi1	AlSi5	as welded
2	AlMgSi1	AlSi5	pwht → T6
3	AlMgSi1	AlMg4.5Mn	as welded
4	AlMg4.5Mn	AlMg4.5Mn	as welded

Table 2: Combinations of base material and filler metals

alloy	position	$R_{po.2}$ [MPa]	R_m [MPa]	A_5 [%]	Z [%]	$\frac{R_{po.2}}{R_{po.2}\ (BM)}$
	HAZ 1	142	200	13.7	50	0.46
	HAZ 2	194	232	13.4	52	0.63
AlMgSi1	HAZ 3	260	280	12.9	44	0.85
	BM	307	328	14.2	41	
PWHT	BM	290	312	12.8	41	
AlMg4.5Mn	BM	166	300	20.3		
	WM	152	285	22.2	33	0.92
AlSi5	WM	91	197	18.4	33	0.30
PWHT	WM	188	242	13.2	25	0.65

Table 3: Strength properties of BM, HAZ and WM of real welds

position	T_{max}	HV 1	condition	$R_{po.2}$ [MPa]	R_m [MPa]
1 (HAZ 1)	550	78	underaged	141	246
2 (HAZ 1)	430	55	very overaged	103	180
3 (HAZ 2)	320	82	overaged	226	256
4 (HAZ 3)	250	106	slightly overaged	281	299

Table 4: Mechanical properties of weld thermal simulated specimens for base material AlMgSi1

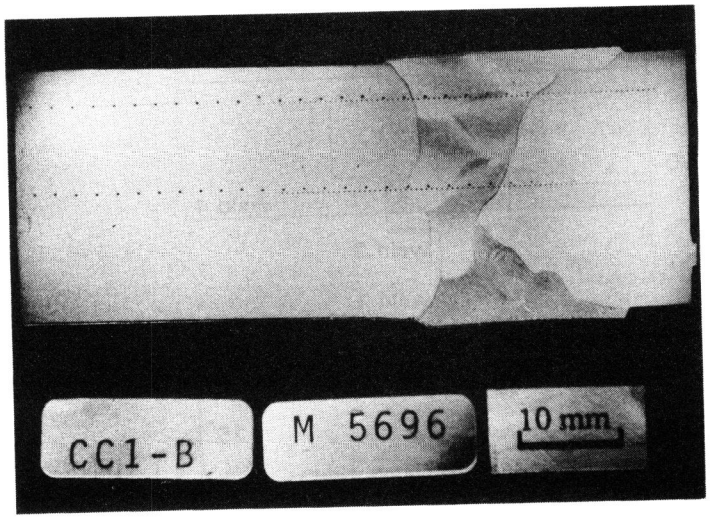

Fig. 1: Micrograph of a section through weld 1 (AlMgSi1/AlSi5, etched 5 % NaOH)

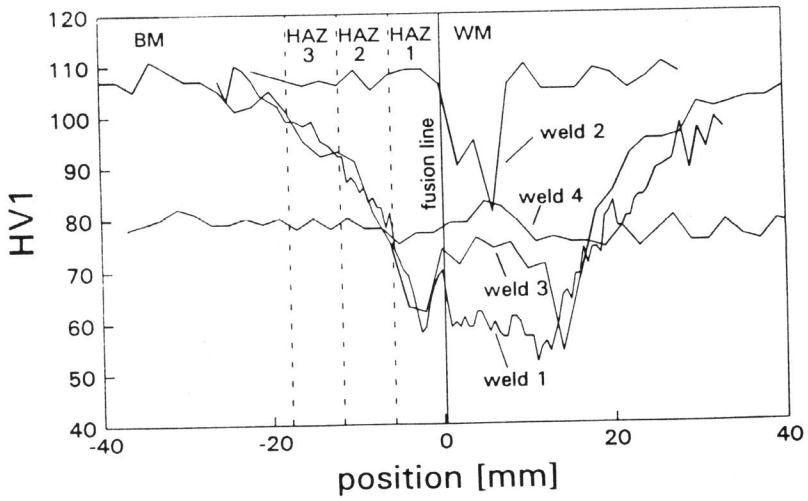

Fig. 2: Vicker's hardness profiles of the welds taken at the center of the plate thickness

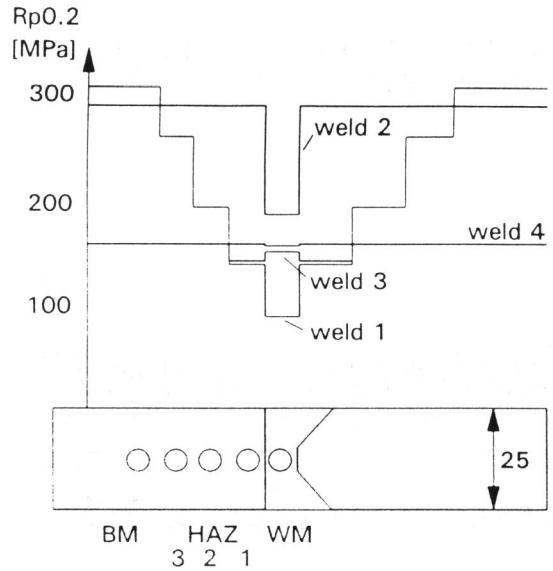

Fig. 3: Strength mismatch (schematic) in the weld region and extraction of tensile specimens - see table 3

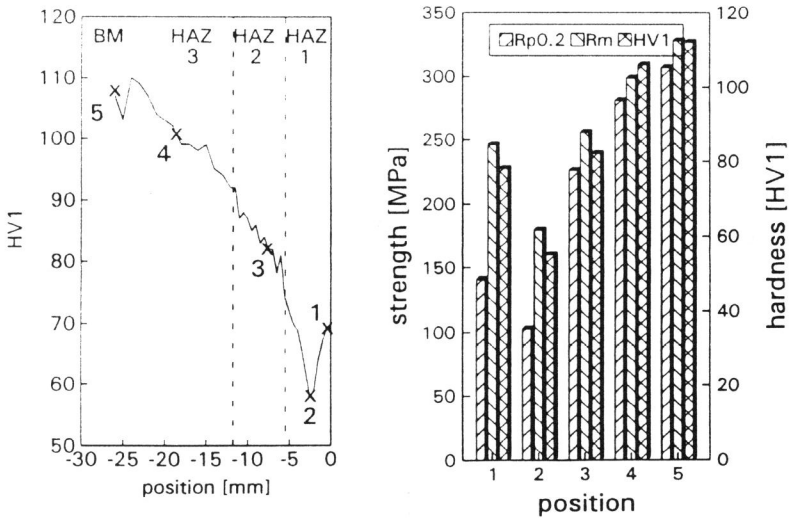

Fig. 4: a) Selected positions in the HAZ (schematic) of weld 1 (AlMgSi1/AlSi5) for weld thermal simulation
b) Hardness and strength of simulated specimens

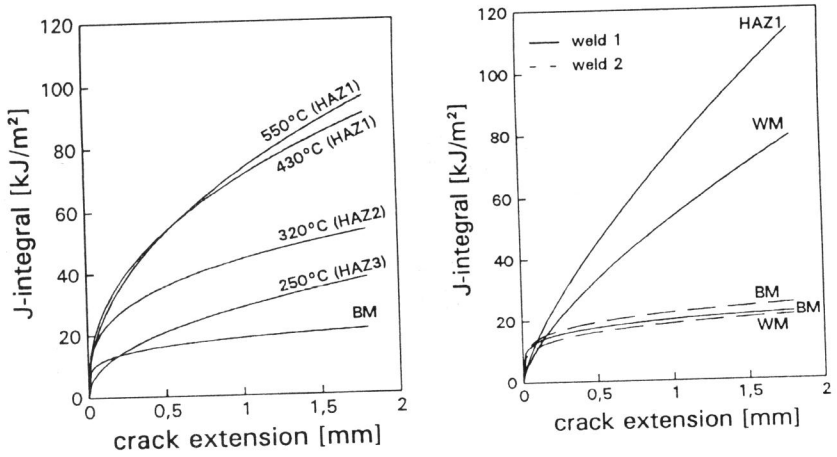

Fig. 5: a) Crack resistance curves for AlMgSi1 weld thermal simulated to different peak temperatures (SE(B)-specimens, 20 x 20 mm, a/W = 0.5)
b) Crack resistance curves for weld 1 and weld 2 (SE(B)-specimens 20 x 40 mm, a/W = 0.1, oriented TL with crack positions in WM, HAZ 1 and BM)

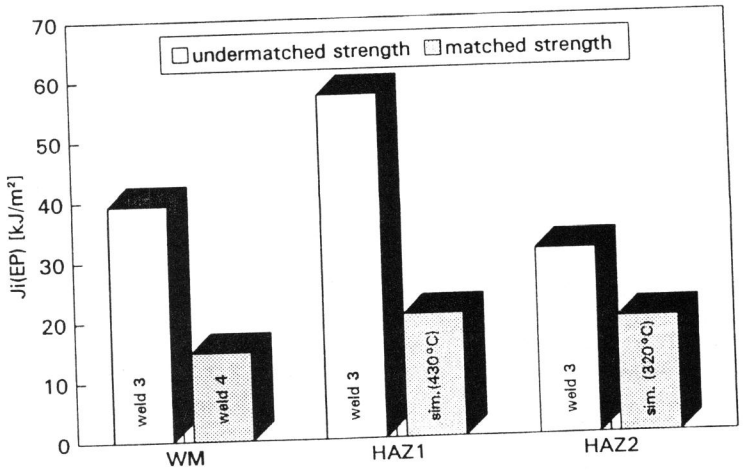

Fig. 6: Fracture toughness J_i at onset of stable crack growth determined by DC-potential method (through thickness cracks a/W = 0.5)

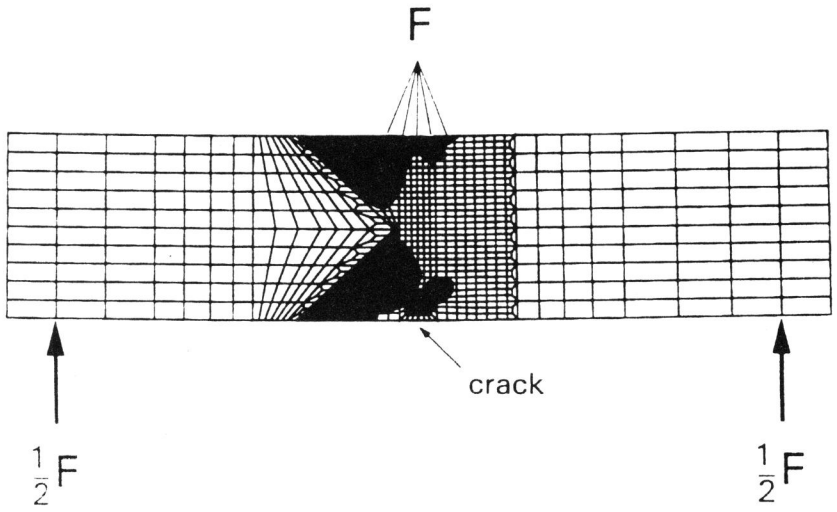

Fig. 7: Plastic zone (black area) in the FE-model (2D) of a loaded SE(B)-specimen of weld 1 with a short through thickness crack in WM (LLD = 0.5 mm)

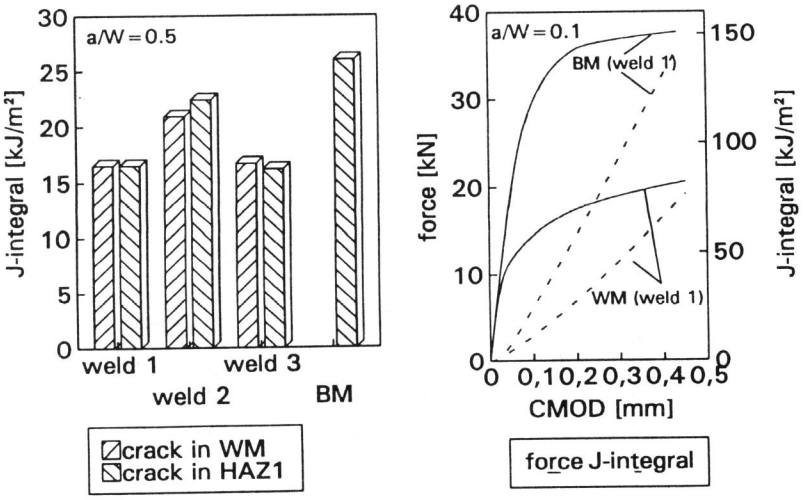

Fig. 8: Loading parameters (force F, J-integral) determined numerically (left fig.: CMOD = 0.3 mm)